

## PRESSURE DEPENDENCE OF CRYSTAL STRUCTURE AND IONIC CONDUCTIVITY ON COMPOSITE GLASS (AgI)<sub>0.7</sub>(AgPO<sub>3</sub>)<sub>0.3</sub>

Supandi Suminta, Evvy Kartini, Mardiyanto and Wisnu Ari Adi  
Centre for Technology of Industrial Nuclear Materials -BATAN

### ABSTRACT

**PRESSURE DEPENDENCE OF CRYSTAL STRUCTURE AND IONIC CONDUCTIVITAS ON COMPOSITE GLASS (AgI)<sub>0.7</sub>(AgPO<sub>3</sub>)<sub>0.3</sub>.** The superionic composite glass, (AgI)<sub>0.7</sub>(AgPO<sub>3</sub>)<sub>0.3</sub> has been successfully synthesized by melt quenching method. The crystal structure of coin type composite glass at various pressure of 100, 300 and 700 kg/cm<sup>2</sup> have been measured by using an X-ray Diffractometer at PTBIN-BATAN. The X-ray diffraction pattern shows some Bragg peaks correspond to the crystalline  $\gamma$ -AgI. The increasing of pressure result the peaks become broaden and shift to the lower angle. This indicates that the crystal size is decreasing and the microstrain is increasing. Three strong peaks at (111), (220) and (311) have been analyzed by using a Gaussian Fitting. Based on calculation, crystal size (D) of (AgI)<sub>0.7</sub>(AgPO<sub>3</sub>)<sub>0.3</sub> at pressures of 100, 300 and 700 kg/cm<sup>2</sup> are 1114 Å, 13165 Å and 7240 Å respectively, while microstrain values ( $\eta$ ) are  $4 \times 10^{-3}$  (1),  $7.5 \times 10^{-3}$  (4) and  $8 \times 10^{-3}$  (4). The composite glass (AgI)<sub>0.7</sub>(AgPO<sub>3</sub>)<sub>0.3</sub> crystal structures at pressures of 100, 300 and 700 kg/cm<sup>2</sup> have been analyzed by using a Rietveld method. The refinement results show that the peaks correspond to  $\gamma$ -AgI phase with a symmetry space group F-4 3 m No. 216, FCC, with the lattice constant namely 6.518(3), 6.508(3) and 6.506Å(2) at a pressure of 100, 300 and 700 kg/cm<sup>2</sup> respectively. The increasing of microstrain ( $\eta$ ), and crystal size (D) and the decreasing of lattice constant (a) will increase the ionic mobility, thus increasing the ionic conductivity. The function of pressure on melt  $\gamma$ -AgI phase into glass matrix AgPO<sub>3</sub> decreases the lattice constant and the crystal size, cause the increasing of microstrain broadening and ionic conductivity

**Keyword :** Microstrain, Particle size, Composite glass, Refinement and Rietveld Analysis

### INTRODUCTION

Recently there has been a rapid technology development of electronic instruments and computers. Due to this reason, the availability of small size power source such as solid state batteries are strongly needed. Some researchers in the field of solid state physics have been working hard in producing superionic conductor due to its promising applications in batteries and sensors [1]. This material can work at room or at higher temperatures. Our research team has been working to contribute in fulfilling the requirement. The works were started by studying one of the components of the batteries i.e. the glass based superionic electrolyte (AgI)<sub>x</sub>(AgPO<sub>3</sub>)<sub>1-x</sub> [2]. The working temperature of the electrolyte varies with the amount of doping salt AgI. The glass transition temperatures are in the region of 40 to 230 °C [3], and it depends on the amount of the AgI dopant. It has been found that the higher the amount of the dopant the lower the glass transition temperature [1]. The maximum solubility of AgI dopant is  $x=0.57$  [4]. Based on our previous results, the ionic conductivity increases with the increase in the

concentration of the dopant AgI and reaches the maximum conductivity when the value of x is approximately 0.6 [5]. The addition of dopant above the maximum solubility causes the conductivity to decrease. This may be caused by the clustering of dopant AgI which resists the movement of both  $\text{Ag}^+$  and  $\text{I}^-$ .

The electrical conductivity within the solid occurs via mobile  $\text{Ag}^+$  ions in the silver iodine regions.. The superionic conductivity increases with increasing concentration of silver iodine until X reaches about 0.55; beyond this level there is precipitation of nearly pure crystalline AgI and the glass component of the sample does not change greatly [6]. Function of pressure of coin type composite glass from melt  $\gamma$ -AgI phase into glass matrix  $\text{AgPO}_3$ , increases ionic conductivity significantly[7]

Based on the above results, the ionic conductivity of saturated glass based  $(\text{AgI})_{0.7} (\text{AgPO}_3)_{0.3}$  electrolyte can be improved by dispersing the dopant AgI clusters via the pressure effect. This paper presents the results of microstrain analysis of glass based  $(\text{AgI})_{0.7} (\text{AgPO}_3)_{0.3}$  electrolyte and the relation between the microstrain with the superionic conductivity.

## BASIC THEORY

Crystal size is seen as a type of defect i.e. a deviation from the crystal of infinite extent and perfect atomic periodicity. Other types of defects are dislocation and subgrains which have important consequences in the diffraction. A crystal with mosaic structure does not have its atoms which are arranged perfectly extending from one side of the crystal to the other. The lattice is broken up into a number of smaller blocks which are slightly disoriented one from another as shown in the Figure 1 below.

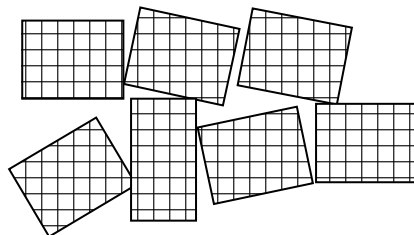


Figure 1.

One of the disorientation effects can be seen as the variation of the diffraction of a parallel monochromatic beam from the single crystal which occur not only at an angle of incidence  $\theta$  but at angle  $\theta + \Delta\theta$ . In the real crystal, whether single crystals or individual grains in a polycrystalline aggregate, has a substructure defined by the dislocations present. The density

of these dislocations is not uniform so that they tend to group themselves into walls surrounding small volumes having a low dislocation density.

Diffraction peaks are influenced by strain. The strain is caused by two types of stresses namely microstresses and macrostresses. If the stress vary from one grain to another, it is called a microstress and corresponds to microstrain. On the other hand when the stress is quite uniform over large distances, it is then referred to as macrostress. The effect of two types of strains is illustrated in Figure 2.

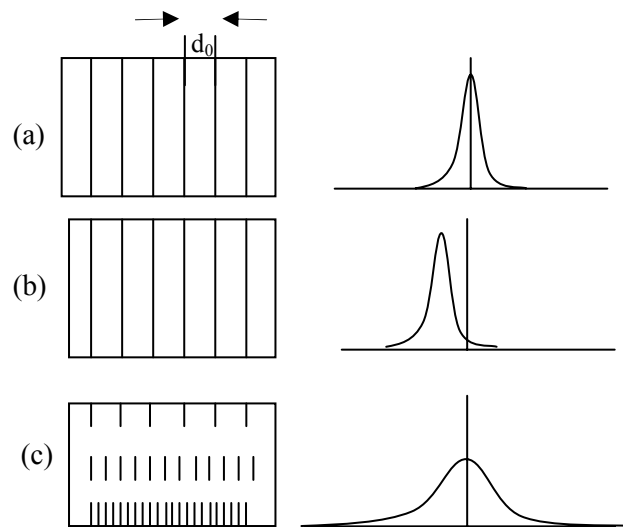


Figure 2. Effect of uniform and non-uniform strain on the diffraction position (a). No strain (b). Uniform strain (c). Non-uniform strain.

Figure 2.b shows that the diffraction line shifts to the left side due to the uniform tensile strain at the right angle to the diffraction planes so that the spacing becomes larger than  $d_0$ . By bending the grain, the strain becomes non-uniform. The spacing on the upper side becomes larger than  $d_0$  and on the other side the spacing becomes smaller. The effect of the non-uniform strain on the grain is that the diffraction line is broadened as shown in Figure 2.c.

Electronics and ionic conductivity are strongly influenced by the defect inside of the material [8]. In order for an ion to move through a crystal the ion must hop from an occupied site to a vacant site. This phenomena will occur if defects are present in the crystal. In general, there are two simplest types of point defects namely Schottky and Frenkel defects. This model is limited to systems with a simple defect structure and most advances have come from molecular dynamic simulations [9].

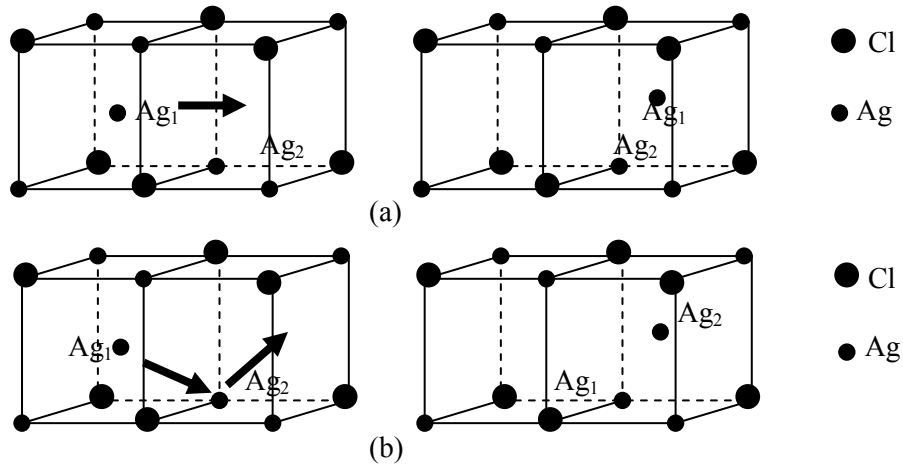


Figure 3. Ion migration (a). Direct interstitial jump (b). Interstitialcy mechanism.

### Cubic Structure, Micro Strain and Crystal Size

The various sets of planes in a lattice have various value of interplanar spacing. The planes of large spacing have low indices and pass through a high a density of lattice points, whereas the reverse is true of plans of small spacing. The interplanar spacing ( $d_{hkl}$ ) is a fungtion both of the planes indices (hkl) and lattice constants ( $a, b, c, \alpha, \beta$  and  $\gamma$ ). The exact relation depends on the crystal system invold and for cubic structure takes on the relation as Equation (1) and (2)

$$\lambda = 2d \sin \theta \quad (1)$$

$$d_{hkl} = \frac{a}{\sqrt{h^2 + k^2 + l^2}} \quad (2)$$

Where :  $d$  is the interplanar spacing;  $a$  is lattice constant;  $h, k, l$  are planes indeces;  $\lambda$  is the wavelength;  $\theta$  is the diffraction angle.

When the size of the individual crystals is less then about  $0.1 \mu\text{m}$  ( $100 \text{ nm} = 1000 \text{ \AA}$ ), the term “particle size” is usually used, but the term “crystallite size” is more precise. Crystals in this size range cause broadening of the Debye rings, the extent of the broadening being given by :

$$B = \frac{0.94\lambda}{D \cos \theta} \quad (3)$$

The analysis of XRD lines was carried out assuming that the full width at half maximum (B) of the lines, after instrumental correction, is due to changes in the particle size and any inhomogeneous mechanical micro strain. In this case, the full width at half maximum (B) in terms of The Bragg angle can be written as equation (4) and (5) :

$$\frac{B \cos \theta}{\lambda} = \frac{0.94}{D} + 2\eta \frac{\sin \theta}{\lambda} \quad \text{or} \quad (4)$$

$$B \cos \theta = \frac{0.94\lambda}{D} + \eta \sin \theta \quad (5)$$

Where : B is the full width at half maximum,  $\lambda$  is the wavelength;  $\theta$  is the diffraction angle,  $D$  is particle size and  $\eta = -2\Delta d/d$  is the micro strain due to inhomogeneous change in d-spacing or lower angle.

In the preceding sections crystal size was seen as a type of defect, i.e., a deviation from the crystal of infinite extent and perfect atomic periodicity assumed in the derivation of the exact equation for the diffractometer is

$$I = |F|^2 p \left( \frac{1 + \cos^2 2\theta}{\sin^2 \theta \cos \theta} \right) e^{-2M} \quad (6)$$

In this equation  $e^{-2M}$  is inserted as a temperature factor and the value of  $e^{-2M}$  can be determined from Figure 4-21 in [10]. Where I = relative integrated intensity (arbitrary units), F = structure factor, p = multiplicity factor, and  $\theta$  = Bragg angle.

Dislocations and subgrains are another type of defect which have important consequences in diffraction.

## EXPERIMENTAL

Superionic glasses  $(\text{AgI})_x(\text{AgPO}_3)_{1-x}$  were prepared at PTBIN-BATAN Laboratory as described elsewhere [5]. For the AgI-doped glasses (with  $x = 0.7$ ), mixtures of AgI (purity 99.9% Aldrich),  $\text{AgNO}_3$  (99.9% Alfa Aesar) and  $\text{NH}_4\text{H}_2\text{PO}_4$  (98% (Caledon)) were heated up to 700 °C and quenched rapidly into liquid nitrogen. Dark – yellow transparent glasses was obtained for superionic composite glass  $(\text{AgI})_{0.7}(\text{AgPO}_3)_{0.3}$  [2]. The quality of coin-type samples was measured by X-ray diffraction. The patterns show a few peaks on the amorphous background for sample at a pressure of 100 kg/cm<sup>2</sup> indicating that the sample has been partially crystallized. The x-ray diffraction measurements were performed for all as-quenched glasses by using a Philips instrument at the PTBIN - BATAN, Indonesia. Detail of the experimental procedure to obtain coin-type samples have been described elsewhere [3].

Figure 4 shows the X-ray diffraction patterns of superionic composite glasses  $(\text{AgI})_{0.7}(\text{AgPO}_3)_{0.3}$  with  $P = 100, 300, \text{ and } 700 \text{ kg/cm}^2$ . For  $(\text{AgI})_{0.7}(\text{AgPO}_3)_{0.3}$  contains a mixture of partially crystalline and partially glass sample and it is called a superionic composite-glass.

The patterns, showed a few peaks on the amorphous background for samples at various pressures for  $100 \text{ kg/cm}^2$  showing that the sample has been partially crystallized, while for pressures of  $300 \text{ and } 700 \text{ kg/cm}^2$ , the peak width on the amorphous background is getting broaden and the intensity decreases.

Crystal structure refinement of  $\gamma\text{-AgI}$  phase in the composite glass  $(\text{AgI})_{0.7}(\text{AgPO}_3)_{0.3}$  has been performed using a Rietveld analysis using RIETAN program, in order to be able to explore the structure of the crystal and to prove that  $\gamma\text{-AgI}$  phase is available in the composite glass  $(\text{AgI})_{0.7}(\text{AgPO}_3)_{0.3}$ . In this study, a Face Centre Cubic (FCC), unit cell with space symmetry  $Fm\bar{3}m$  No. 216 was assigned to this compound based on the systematic absence of Bragg reflection.

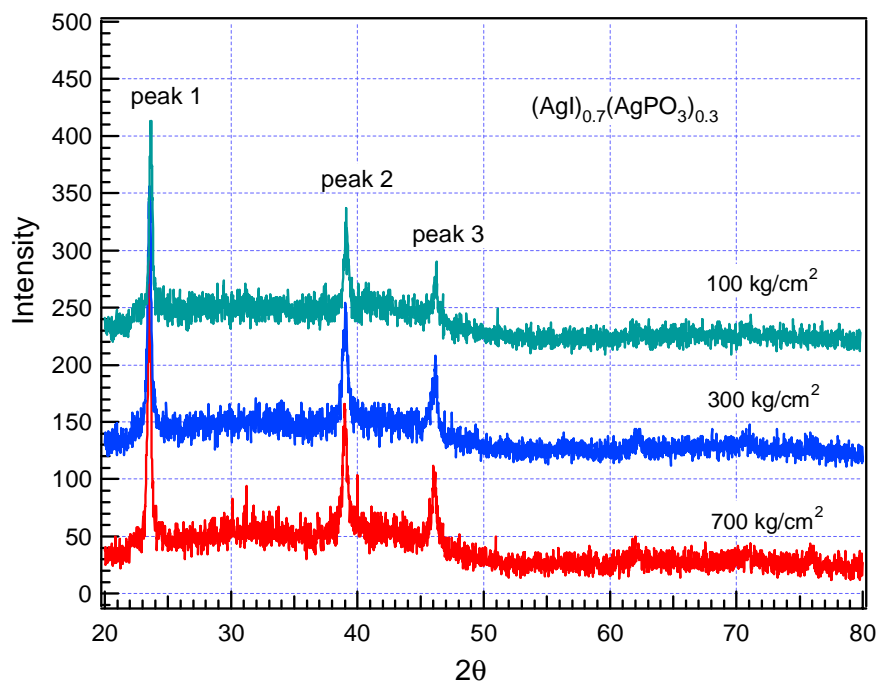


Figure 4. XRD Patterns of  $(\text{AgI})_{0.7}(\text{AgPO}_3)_{0.3}$  at pressure  $100, 300 \text{ and } 700 \text{ kg/cm}^2$  (raw data).

## RESULTS AND DISCUSSION

### Gaussian fitting

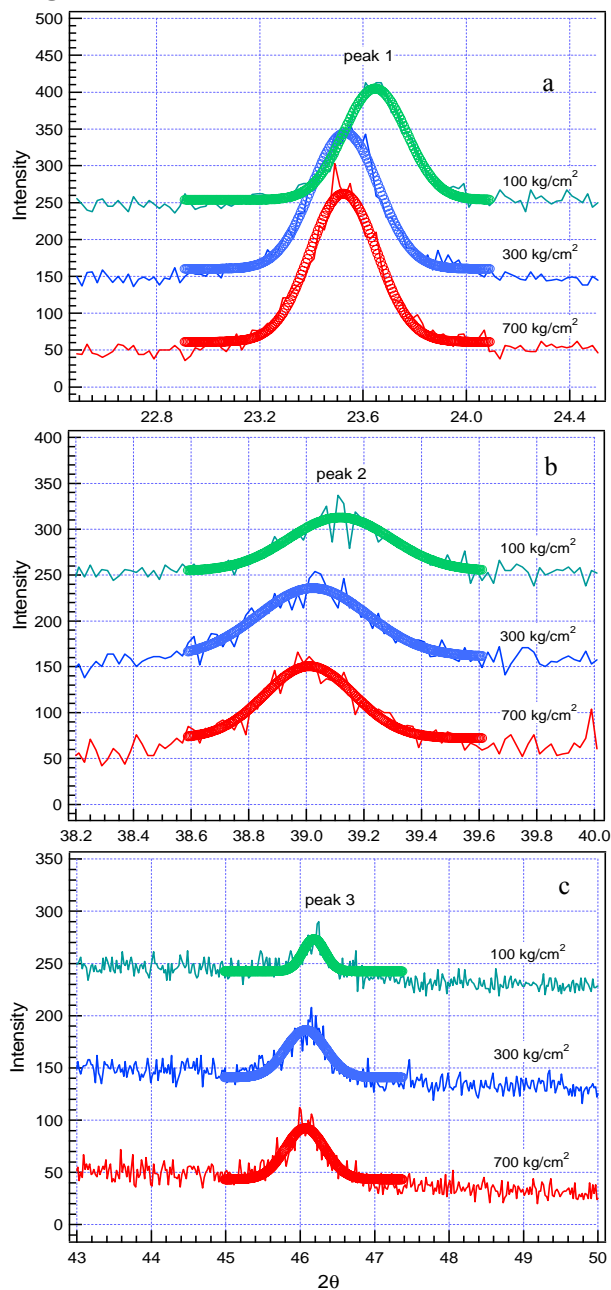


Figure 5. Fitting analysis to the three Bragg peaks of  $(\text{AgI})_{0.7}(\text{AgPO}_3)_{0.3}$  at three different pressures (100, 300 and 700 kg/cm<sup>2</sup>), a) Peak 1, b) peak 2 and c) peak 3.

Figure 5. Shows results of fitting analysis to the Bragg peaks of  $(\text{AgI})_{0.7}(\text{AgPO}_3)_{0.3}$  at three different peaks (peak 1, 2 and 3) and at different pressures 100, 300 and 700  $\text{kg/cm}^2$  respectively. However, through close inspection, there are changes in the positions, intensities and width of the Bragg peaks (peak 1, 2 and 3) with different pressures due to the different stress and strain, as shown in Figure 5. Theoretically, when a polycrystalline piece of material is deformed elastically in such manner that the strain is uniform over relatively large distances, the lattice plane spacings in the constituent grains change from their stress-free value (at normal stress) to some new value corresponding to the magnitude of the applied stress. This new spacing being essentially constant from one grain to another for any particular set of planes similarly oriented with respect to the stress. This uniform macrostrain causes a shift of the diffraction lines to the new  $2\theta$  positions. In fact, the given pressures cause not only uniform strain but also nonuniform microstrain. This nonuniform microstrain causes a broadening of the corresponding diffraction line. On the other hand, the deformed sub-grains increase the integrated intensity of the diffracted beam relative to that of an ideally perfect crystal. The results of the experiment agree with the theory.

Table 1. FWHM and  $2\theta$  data of Gaussian fitting analysis results of  $(\text{AgI}_{0.7})(\text{AgPO}_3)_{0.3}$  (pressure dependence)

No.	Pressure ( $\text{kg/cm}^2$ )	$2\theta$			FWHM ( $\beta$ )		
		Peak 1	Peak 2	Peak 3	Peak 1	Peak 2	Peak 3
1	100	23.647 $\pm 0.003$	39.12 $\pm$ 0.01	46.19 $\pm 0.01$	0.172 $\pm 0.005$	0.25 $\pm 0.03$	0.27 $\pm 0.02$
2	300	23.531 $\pm 0.003$	39.024 $\pm 0.009$	46.08 $\pm 0.01$	0.183 $\pm 0.003$	0.27 $\pm 0.02$	0.38 $\pm 0.02$
3	700	23.524 $\pm$ 0.003	39.011 $\pm 0.007$	46.05 $\pm$ 0.01	0.185 $\pm 0.006$	0.28 $\pm 0.01$	0.39 $\pm 0.02$

Table 2. Reflection Bragg data and particle size by Gaussian Fitting analysis

Pressure ( $\text{kg/cm}^2$ )	Peak	$\theta$	FWHM ( $\beta$ )		$\beta \cos \theta$	$\sin \theta$	D ( $\text{\AA}$ )	Strain ( $\eta$ )
			( $2\theta^\circ$ )	(radian)				
100	Peak 1	11.823	0.172	0.0030	0.0029	0.205	1114	$4 \times 10^{-3}$
	Peak 2	19.56	0.25	0.0044	0.0041	0.335		
	Peak 3	23.095	0.27	0.0047	0.0043	0.392		
300	Peak 1	11.765	0.183	0.0032	0.0031	0.2039	13165	$7.5 \times 10^{-3}$
	Peak 2	19.512	0.27	0.0047	0.0044	0.3340		
	Peak 3	23.04	0.38	0.0066	0.0061	0.3914		
700	Peak 1	11.762	0.185	0.0032	0.0031	0.2038	6582	$8 \times 10^{-3}$
	Peak 2	19.505	0.28	0.0049	0.0046	0.3339		
	Peak 3	23.025	0.39	0.0068	0.0062	0.3911		
$0.94 \times \lambda = 0.94 \times 1.540562 = 1.44812828$								

The results of the fitting analysis to the Bragg peaks in  $(\text{AgI})_{0.7}(\text{AgPO}_3)_{0.3}$  at three different pressures are listed in table 1 and 2. With increasing pressure, in general the peak shifts to the lower angle at about  $\sim 0.1^\circ$ , while the width (FWHM) increases about  $0.01^\circ$  and  $0.1^\circ$  for peak 1, 2, and peak 3, respectively.  $\eta = -2\Delta d/d$  is the micro strain due to inhomogeneous change in d-spacing.

Equation (5) :

$$\beta \cos \theta = \frac{0.94\lambda}{D} + 2\eta \sin \theta$$

and is similar to the linear equation ;  $y = a + bx$

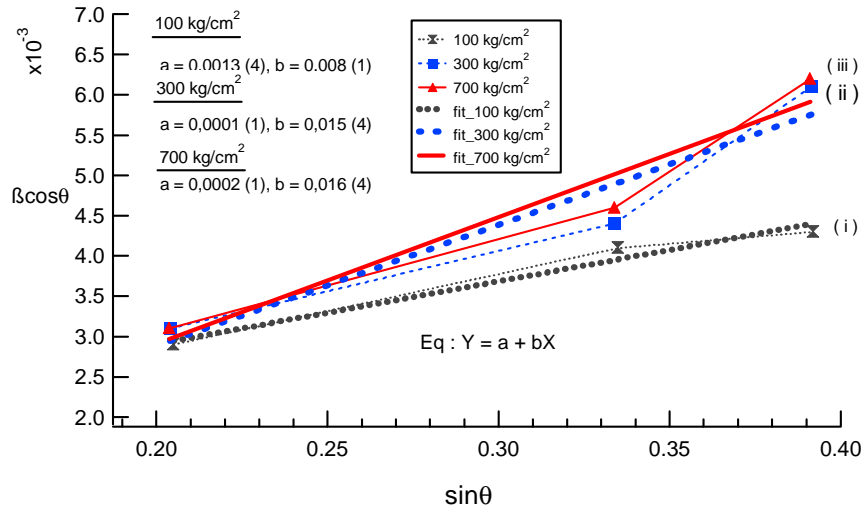


Figure 6. Plot of  $\beta \cos \theta$  versus  $\sin \theta$  as a function of pressure, curve (i) pressure for  $100 \text{ kg/cm}^2$ , (ii) pressure for  $300$  and (iii) pressure for  $700 \text{ kg/cm}^2$ .

Separation of size and strain components can be done by plotting  $\beta \cos \theta$  as a function of  $\sin \theta$  ( Figure 6); this type of plot is known as a Scherrer's formula (5) and implicitly assumes that the peak shapes are Lorentzian. Rearranging the terms of Equation (5) produces :

$$\beta \cos \theta = \frac{0.94\lambda}{D} + 2\eta \sin \theta$$

Where  $\beta$  is the half-width of a given diffraction peak,  $\lambda$  is the wavelength of X-ray used,  $\eta$  is a measure of lattice strain,  $\theta$  is the Bragg angles and  $D$  is the particle size. Figure 6 shows the relation between  $\beta \cos \theta$  and  $\sin \theta$  for the diffraction peaks of  $\gamma$ -AgI in the superionic composite glass

(AgI)<sub>0.7</sub>(AgPO<sub>3</sub>)<sub>0.3</sub>. The values of  $\eta$  in Equation (5), the measurement of lattice strain, are obtained from the slopes of the plots. It is apparent that  $\gamma$ -AgI in the composites at pressure for 300 and 700 kg/cm<sup>2</sup> have larger lattice strain compared with the the composite at pressure for 100 kg/cm<sup>2</sup>. Such a large lattice strain of  $\gamma$ -AgI at pressure (300 and 700 kg/cm<sup>2</sup>) must be caused by stress at the interface between the AgI crystals and the glass matrix during rapid quenching and pressing.

If size broadening is the only significant contribution to peak width, then  $\beta \cos \theta$  is a constant for all peak. If strain broadening is important contribution  $\beta \cos \theta$  is a linear function of  $\sin \theta$  Equation (4) and (5) as show in Figure 6.

Figure 6. shows data for coin-type superionic composite glass (AgI)<sub>0.7</sub>(AgPO<sub>3</sub>)<sub>0.3</sub> in three conditions pressure : 100 (normal pressure), 300 and 700 kg/cm<sup>2</sup>. It is expected that the coin-type superionic composite glass (AgI)<sub>0.7</sub>(AgPO<sub>3</sub>)<sub>0.3</sub> with the pressure of 100 kg/cm<sup>2</sup> (normal pressure) produces less microstrain and higher crystalline size in superionic composite glass (AgI)<sub>0.7</sub>(AgPO<sub>3</sub>)<sub>0.3</sub>. The corresponding value of microstain and crystalline size are  $4 \times 10^{-3}$  and 1114 Å respectively. While the microstrain and crystalline size for the other two pressures (i.e. 300 and 700 kg/cm<sup>2</sup>) are  $7.5 \times 10^{-3}$  and  $8 \times 10^{-3}$ , and 13165 Å and 6582 Å, respectively (Table 3).

### Structure Determination of $\gamma$ -AgI in Glassy Electrolyte (AgI)<sub>0.7</sub>(AgPO<sub>3</sub>)<sub>0.3</sub>

The refinement results of the three Bragg peaks show that the position of the peak shifts to lower angle, the peak width is getting broaden as shown in Table 2

Figure 7 shows Rietveld refinement X-ray diffraction Patterns of  $\gamma$ -AgI in (AgI)<sub>0.7</sub>(AgPO<sub>3</sub>)<sub>0.3</sub>, at 100, 300 and 700 kg/cm<sup>2</sup>. The solid light blue lines (—) are calculated intensities, the mark red lines ( + ) are observed intensities. The lowest curve of Figure 7.a,b, and c indicates the different between the calculated and observed patterns, respectively. The green vertical lines ( | ) (Figure 7.a, b and c ) mark the position of possible Bragg's diffraction of  $\gamma$ -AgI phase.

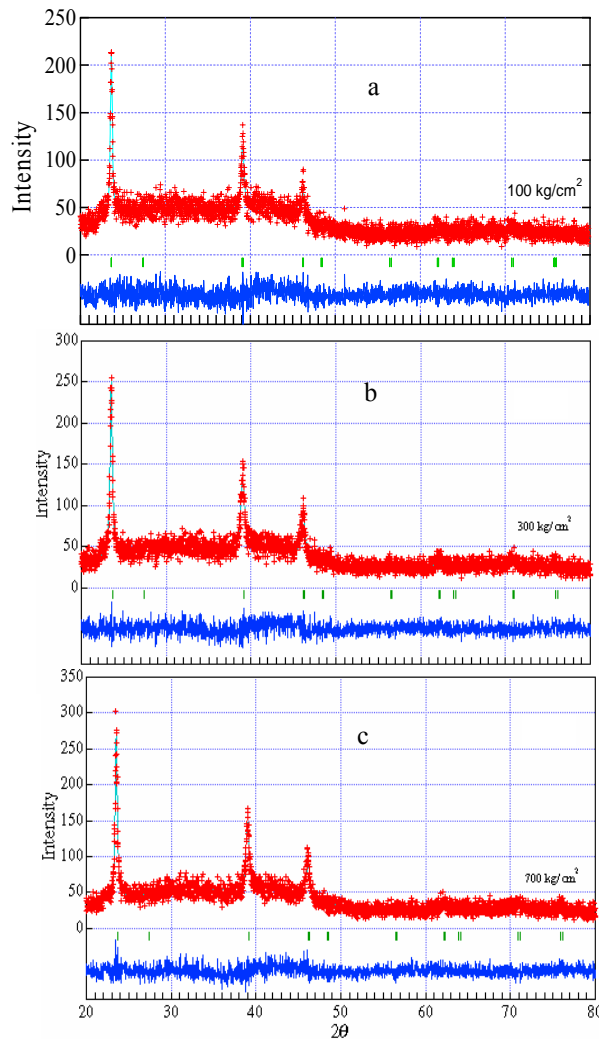


Figure 7. Rietveld refinement X-ray diffraction Patterns of  $(\text{AgI})_{0.7}(\text{AgPO}_3)_{0.3}$  at pressures : a)  $100 \text{ kg/cm}^2$ ; b) pressure  $300 \text{ kg/cm}^2$ ; and c)  $700 \text{ kg/cm}^2$ , and refinement fits.

Further crystal structure refinement of  $\gamma\text{-AgI}$  in the composite glass  $(\text{AgI})_{0.7}(\text{AgPO}_3)_{0.3}$  has been performed using a Rietveld analysis using RIETAN program. In this study, a Face Centre Cubic (FCC) unit cell with space symmetry F-4 m n No. 216 was assigned to this compound based on the systematic absence of Bragg reflection. Figure 7 shows refinement result, which is in satisfactory agreement between observed and calculated intensity (R factor :  $R_{\text{wp}} = 17.85 \%$ ,  $S = 1.0869$ ,  $R_p = 16.45 \%$ ,  $R_e = 19.06 \%$ ). The structural parameters and lattice parameters of  $\gamma\text{-AgI}$  : g, x, y, z and B are isotropic as shown in table 3

Table 3. Data of Refinement result of  $\gamma$ -AgI

<b>1. Pressure 100 kg/cm<sup>2</sup></b>						
Atom/Ion	Wyckoff	g	x	y	z	B <sub>iso</sub>
Ag <sup>+</sup>	4b	1	0.0	0.0	0.0	8(2)
I <sup>-</sup>	4a	1	0.25	0.25	0.25	3(1)
Space group	: F-4 3 m No. 216					
Crytal system	: Cubic FCC					
phase	: $\gamma$ -AgI (gamma silver iodide)					
lattice const.	: a =b=c = 6.518(3) Å					
R. factor	: Rwp = 17.85 %, Rp = 13.78 %					
<b>2. Pressure 300kg/cm<sup>2</sup></b>						
Atom/Ion	Wyckoff	g	x	y	z	B <sub>iso</sub>
Ag <sup>+</sup>	4b	1	0.0	0.0	0.0	7(1)
I <sup>-</sup>	4a	1	0.25	0.25	0.25	2.0(7)
Space group	: F-4 3 m No. 216					
Crytal system	: Cubic FCC					
phase	: $\gamma$ -AgI (gamma silver iodide)					
lattice const.	: a =b=c = 6.508(3) Å					
R. factor	: Rwp = 17.16 %, Rp = 13.41 %					
<b>3. Pressure 700kg/cm<sup>2</sup></b>						
Atom/Ion	Wyckoff	g	x	y	z	B <sub>iso</sub>
Ag <sup>+</sup>	4b	1	0.0	0.0	0.0	7(1)
I <sup>-</sup>	4a	1	0.25	0.25	0.25	1.9(6)
Space group	: F-4 3 m No. 216					
Crytal system	: Cubic FCC					
phase	: $\gamma$ -AgI (gamma silver iodide)					
lattice const.	: a =b=c = 6.506(2) Å					
R. factor	: Rwp = 17.03 %, Rp = 13.21 %					

Based on the results of the Rietveld analysis using program RIETAN as shown in Table 3, the saturated (AgI)<sub>0.7</sub> (AgPO<sub>3</sub>)<sub>0.3</sub> samples which were pressed under 100, 300, 700 kg/cm<sup>2</sup> resulted in both uniform and non-uniform strain. The AgI grain clusters that were under macrostress contributed to the shifting of the diffraction line to the lower angle. It can be seen from the Table 2 that the bigger the macrostress the lower the 2 $\theta$  angle. On the other hand, the effect of the microstress due to the mechanical pressure also contributed to the dispersion of the grain clusters. There was the possibility that under mechanical stress, the brittle AgI grain clusters in the coin type sample (AgI)<sub>0.7</sub> (AgPO<sub>3</sub>)<sub>0.3</sub> initially did have dislocation effects because of the sliding process. The AgI grain clusters were surrounded by the hard glass base (AgI)<sub>0.7</sub> (AgPO<sub>3</sub>)<sub>0.3</sub> electrolyte. Thus the gliding process was blocked by the electrolyte such that a highly concentrated stress was collected in this area. In this situation, the atomics bonds were under great stress. They stretched beyond their limit and rapture, forming a tiny crack. It can be seen from the Table 2 that these effects resulted in the broadening the peaks.

### Pressure Dependence of Conductivity

By giving the different pressures on the samples two phenomena can be obtained namely the bigger the given pressure the less cavities and the higher the glass links. So that two phenomena provide better ionic conductivity of the AgI based superionic glasses. Fig. 8 shows that by increasing the pressure on the sample the conductance of the  $(\text{AgI})_{0.7}(\text{AgPO}_3)_{0.3}$  glass also increases over the wide range of the frequency from 50 Hz. to 5 MHz. The powder electrolyte glasses were pressed into coin type samples with pressure of 100 kg/cm<sup>2</sup>, 200 kg/cm<sup>2</sup>, 300 kg/cm<sup>2</sup>, 700 kg/cm<sup>2</sup> and their conductivities of 1.65E-05 [S/cm]; 1.01E-04 [S/cm]; 1.32E-4 [S/cm]; 1.63E-4 [S/cm] were obtained when they were measured by using LCR meter at 50 Hz.

If we fit the curves of Fig.8 it seems that each curve can be divided into two parts. These are the linear part over the range of low frequency from 50 Hz to about 6 kHz and the exponential part over the range of frequency higher than 6 kHz. In the linear part the relation between the conductivity and the frequency can stated using the equation :

$$\text{Log } \sigma = S \text{ log } \nu + \sigma_0 \quad (7)$$

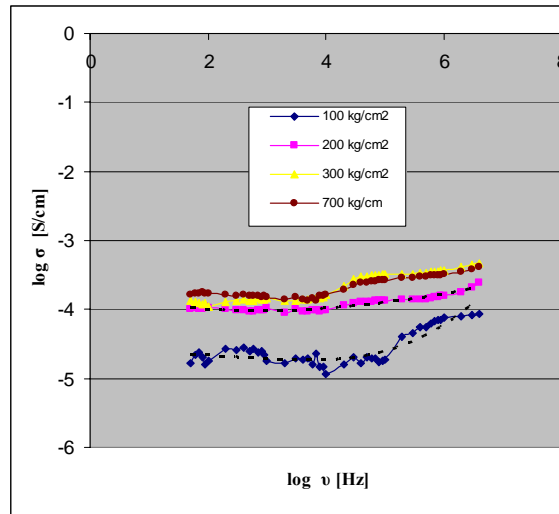


Figure 8. Plot of  $\log \sigma$  [S/cm] versus  $\log \nu$ .

Here  $\sigma_0$  is DC conductivity of the superionic glass. From Figure 8 it can be seen that the slope of the line is close to zero. This means that in this range of frequency the conductivity is not a function of frequency and the movement of the ions is only a hopping process. Meanwhile, in the second part, the conductivity changes with the increase of the frequency. Here the movement of the ions is caused by the vibration of the ions.

## CONCLUSION

The melt-quenched  $(\text{AgI})_{0.7}(\text{AgPO}_3)_{0.3}$ , superionic composite glass has been measured using an X-ray Diffractometer. The X-ray diffraction pattern shows some Bragg peaks that corresponds to the crystalline  $\gamma$ -AgI. The crystal structures at pressure  $P = 100, 300$  and  $700 \text{ kg/cm}^2$  of the composite glass  $(\text{AgI})_{0.7}(\text{AgPO}_3)_{0.3}$  have been analysed by using Rietveld method. The refinement results show that  $\gamma$ -AgI phase has a symmetry space group F-4 3 m No. 216, FCC, with the lattice constant namely  $6.518(3), 6.508(3)$  and  $6.506(2) \text{ \AA}$  for the pressuring of  $100, 300$  and  $700 \text{ kg/cm}^2$  respectively. The microstrain ( $\eta$ ) of the pressure,  $P = 100, 300$  and  $700 \text{ kg/cm}^2$  are  $4 \times 10^{-3}(1), 7.5 \times 10^{-3}(4)$  and  $8 \times 10^{-3}(4)$  respectively. The particle size ( $D$ ) are  $1114, 13165$  and  $7240 \text{ \AA}$  respectively. On the other hand, from the ionic conductivity point of view, the effect of the mechanical pressure dispersed the AgI grain clusters which resulted in the higher ionic conductivity namely from  $1.65 \times 10^{-5} [\text{S/cm}]$  to  $[1.63 \times 10^{-4} [\text{S/cm}]]$ . It is concluded that the doped silver oxysalt glasses based on tetrahedral anions are highly efficient ionic conductors. The function of pressure on melt  $\gamma$ -AgI phase into glass matrix  $\text{AgPO}_3$  decreases the lattice constant and increases the crystal size, thus increasing the microstrain broadening and the ionic conductivity

## ACKNOWLEDGMENT

The authors wishes to thank to Dr. Ridwan and Dr. Pudji Untoro at PTBIN-BATAN for the use of the facilities; Dr. A.Fajar for a helpfull discussion. The authors acknowledge the referee for his constructive criticism and some valuable suggestions for improving the manuscript. This work was supported by the Indonesian International Joint Research Program (RUTI IV), Contract No.6D/Perj/Dep.III/RUTI/PPKI/2005 and No.10/Perj/Dep.III/RUTI/PPKI/I/2006.

## REFERENCES

1. M.F. Collins and E. Kartini, “*Superonic conduction in silver oxysalt-silver salt glasses*”, Transworld Research Network, 37/661 920, Fort P.O., Trivandrum-695 023, Kerala, India, Solid State Ionic, 1(2003) : 157-174 ISBN : 81-7895-069-3
2. A.Purwanto, E. Kartini, T. Kamiyama, A.Hoshikawa, S. Harjo, M.F. Collins and S. Purnama, “*Disappearance of  $\beta$ AgI in  $(\text{AgI})_{0.7} - (\text{NaPO}_3)_{0.3}$  composite at room temperature*” Solid State Ionics 171 (2004) 113 - 119

3. T. Sakuma, Y.Nakamura, M.Hirota, A.Murakami, Y.Ishii, “*Diffuse Scattering from AgBr Application to Rietveld Refinements*”, *Solid State Ionics*, 127 (2000) 295-300
4. E.Kartini, M.F. Collins, “*Nature of the precipitate in (AgI)<sub>0.7</sub>(AgPO<sub>3</sub>)<sub>0.3</sub> glass*”, *Physica B* 276-278 (2000) 476-468
5. E. MUSHAFAAH., Sintesis, ”*Karakterisasi Struktur dan Sifat Termal Pada Bahan konduktor Superionik Berbasis Gelas (Ag<sub>2</sub>S)(AgPO<sub>3</sub>)<sub>1-x</sub>*”, Karya Tulis Jurusan Fisika, FMIPA Institut Pertanian Bogor (2002)
6. B. Wnetrzewski, J.L. Nowinski and W. Jakubowski, “*Nature of the AgI precipitate*”, *Solid State Ionics*, 36, 1989,209-214
7. Mardiyanto, E. Kartini, Gunawan, A. Hindasyah, and M. Ihsan, “*Effect of pressure on the ionic conductivity of (AgI)<sub>0.7</sub>(AgPO<sub>3</sub>)<sub>0.3</sub> glasses*”, *Indonesian Journal of Material Science*, (2007, in press)
8. [http://www.chemistry.ohio-state.edu/~windward/ch754/ionic\\_conductivity.pdf](http://www.chemistry.ohio-state.edu/~windward/ch754/ionic_conductivity.pdf), July 15, 2005
9. T. Takehashi, “*Silver conducting solid electrolytes, Handbook of Solid State Batteries & Capacitors* “, chapter 4, World Scientific Publishing Co. Pte. Ltd., Singapore,1995
10. B.D. Cullity and S.R. Stock, “*Elements of X-ray diffraction*”, Prentice Hall, Upper Saddle River, New Jersey, 2001